

# Supporting Information

## Atomistic Insight into Ion Transport and Conductivity in Ga/Al-Substituted $\text{Li}_7\text{La}_3\text{Zr}_2\text{O}_{12}$ Solid Electrolytes

Fabián A. García Daza<sup>\*1</sup>, Mauricio R. Bonilla<sup>1</sup>, Anna Llordés<sup>2,3</sup>, Javier Carrasco<sup>\*2</sup>, and Elena Akhmatkaya<sup>1,3</sup>

<sup>1</sup>Basque Center for Applied Mathematics, Alameda de Mazarredo 14 (48009) Bilbao, Spain

<sup>2</sup>CIC EnergiGUNE, Albert Einstein 48 (01510) Miñano, Spain

<sup>3</sup>IKERBASQUE, Basque Foundation for Science (48013) Bilbao, Spain

E-mail: fgarcia@bcamath.org; jcarrasco@cicenergigune.com

## S1. Sampling the Potential Energy Distributions of $\text{Ga}_x\text{Al}_{0.2-x}$

In this work, a  $3 \times 3 \times 3$  LLZO supercell (containing 1944 available Li sites, 648 La atoms, 432 Zr atoms, and 2592 O atoms) is considered, with substituent Ga and Al cations confined to the tetrahedral ( $T_d$ ) sites of the structure. There exists an enormous number of conceivable arrangements for the Li, Li vacancies, Al and Ga within the Li sublattice. A simple sampling approach consists of randomly adjusting the Li/Ga/Al/vacancy arrangements according to the desired stoichiometry<sup>1-4</sup>. Accordingly, for each  $x$  in  $\{0.0, 0.1, 0.2\}$ , a total of 10000 random structures of  $\text{Ga}_x\text{Al}_{0.2-x}$  were generated, and those with the lowest total potential energy, PE (electrostatic + short range) for each value of  $x$  were selected for fine-tuning of interatomic parameters and subsequent atomistic simulations. Calculations of the PE on the static structures were performed using LAMMPS<sup>5</sup>. The potential parameters were taken from Jalem et al.<sup>1</sup> for Ga-substituted LLZO, and from Pedone et al.<sup>6</sup> for the Al-O potential. These parameters are reported in Table S1. Figure S1 depicts the resulting PE histograms.

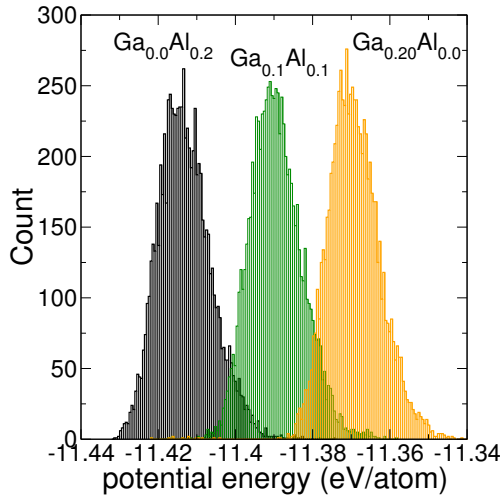


Figure S1: PE histograms for  $\text{Ga}_x\text{Al}_{0.2-x}$ , with  $x$  in  $\{0.0, 0.1, 0.2\}$

## S2. Fine Tuning of the Interatomic Potential

We model the short range interaction between atoms  $i$  and  $j$ ,  $U_{ij}^{\text{vdW}}$ , using the Buckingham potential:

$$U_{ij}^{\text{vdW}} = A_{ij} \exp(-B_{ij} |\mathbf{r}_{ij}|) - \frac{C_{ij}}{|\mathbf{r}_{ij}|^6}, \quad (\text{S1})$$

where  $|\mathbf{r}_{ij}|$  is the distance between particles and  $A_{ij} \geq 0$ ,  $B_{ij} > 0$  and  $C_{ij} \geq 0$  are the Buckingham parameters. Initially, the potential parameters corresponded to those reported by Jalem et al.<sup>1</sup> for Ga-substituted LLZO, and from Pedone et al.<sup>6</sup> for the Al-O potential (Table S1).

Table S1: Buckingham parameters for Ga- and Al-substituted LLZO prior to fine tuning. The values were taken from Jalem et al.<sup>1</sup> for Ga-substituted LLZO, and from Pedone et al.<sup>6</sup> for the Al-O potential.

Interactions	$A$ (eV)	$B$ ( $\text{\AA}^{-1}$ )	$C$ (eV $\text{\AA}^6$ )
Ga <sup>2.1-</sup> - O <sup>1.4-</sup>	13298.83	4.963	0.0
Al <sup>2.1-</sup> - O <sup>1.4-</sup>	7042.593	4.316	101.495
Li <sup>0.7+</sup> - O <sup>1.4-</sup>	876.86	4.110	0.0
La <sup>2.1+</sup> - O <sup>1.4-</sup>	14509.63	4.102	30.83
Zr <sup>2.8+</sup> - O <sup>1.4-</sup>	2153.80	3.439	0.0
O <sup>1.4-</sup> - O <sup>1.4-</sup>	4869.99	4.163	27.22

After fine tuning to match the structural cell parameters reported by Rettenwander et al.<sup>7</sup>, we found that the optimal value of  $B_{\text{Li-O}}$  varies with  $x$ . The variation of the optimal  $B_{\text{Li-O}}$  with  $x$  is shown in Fig. S2.

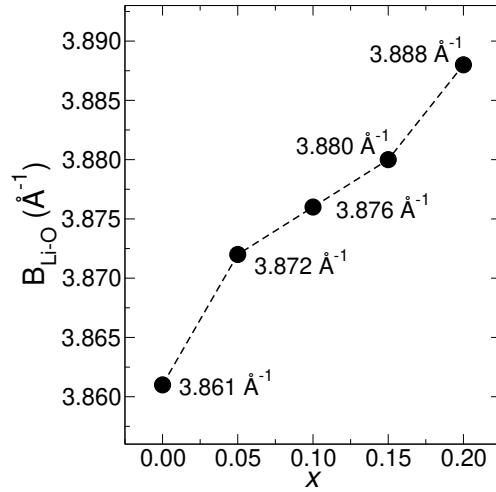


Figure S2: Buckingham parameter  $B_{\text{Li-O}}$  for  $\text{Ga}_x\text{Al}_{0.2-x}$  with  $x$  in  $\{0.0, 0.05, 0.10, 0.15, 0.20\}$ .

### S3. Integrated Autocorrelation Function for LLZO

Sampling efficiency of MD and GSHMC methods can be compared by calculating the integrated autocorrelation function (IACF),

$$\text{IACF}(f(t)) = \int_0^\infty \text{ACF}(f(t)) dt, \quad (\text{S2})$$

where  $f$  is a time dependent property, and, ACF is the autocorrelation function which is defined as

$$\text{ACF}(f(t)) = \langle f(t_0)f(t_0 + t) \rangle_{t_0}. \quad (\text{S3})$$

The IACF in Eq. S2 estimates the time needed, on average, to generate a non-correlated sample. Low IACF values indicate a low correlation between samples, therefore, a more efficient sampling is achieved. For both MD and GSHMC simulations, and considering potential energy as the property of interest, IACFs for  $\text{Ga}_{0.0}\text{Al}_{0.2}$ ,  $\text{Ga}_{0.1}\text{Al}_{0.1}$  and  $\text{Ga}_{0.2}\text{Al}_{0.0}$  systems have been calculated at 233 K, 273 K and 313 K during the equilibration stage in the NVT ensemble (see Table S2)

Table S2: GSHMC and MD IACF values for  $\text{Ga}_x\text{Al}_{0.2-x}$  at different temperatures.

$x$	233 K		273 K		313 K	
	MD	GSHMC	MD	GSHMC	MD	GSHMC
0.0	39.7	4.4	25.9	7.1	11.3	8.8
0.1	29.6	2.1	19.0	2.6	7.6	2.9
0.2	19.4	1.5	10.7	1.8	6.0	2.1

### S4. Thermal Expansion in Al/Ga-Containing LLZO Garnet

Thermal expansion/contraction of Al/Ga-substituted LLZO has been calculated for temperatures between 193 K and 313 K for  $\text{Ga}_{0.0}\text{Al}_{0.2}$ ,  $\text{Ga}_{0.1}\text{Al}_{0.1}$  and  $\text{Ga}_{0.2}\text{Al}_{0.0}$ . Our calculations reveal that increasing the Ga content in  $\text{Ga}_x\text{Al}_{0.2-x}$  garnets produce a subtle increase in the lattice parameter at all temperatures (see Fig. S3).

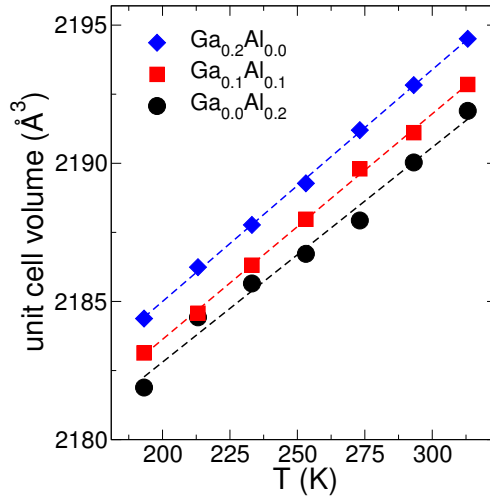


Figure S3: Thermal expansion in  $\text{Ga}_x\text{Al}_{0.2-x}$ , for  $x$  in  $\{0.0, 0.1, 0.2\}$

## References

- [1] R. Jalem, M. Rushton, W. Manalastas, M. Nakayama, T. Kasuga, J. A. Kilner, and R. W. Grimes, “Effects of Gallium Doping in Garnet-Type  $\text{Li}_7\text{La}_3\text{Zr}_2\text{O}_{12}$  Solid Electrolytes,” *Chem. Mater.*, vol. 27, no. 8, pp. 2821–2831, 2015.
- [2] L. J. Miara, W. D. Richards, Y. E. Wang, and G. Ceder, “First-Principles Studies on Cation Dopants and Electrolyte|Cathode Interphases for Lithium Garnets,” *Chem. Mater.*, vol. 27, no. 11, pp. 4040–4047, 2015.
- [3] L. Lander, M. Reynaud, J. Carrasco, N. A. Katcho, C. Bellin, A. Polian, B. Baptiste, G. Rousse, and J.-M. Tarascon, “Unveiling the Electrochemical Mechanisms of  $\text{Li}_2\text{Fe}(\text{SO}_4)_2$  Polymorphs by Neutron Diffraction and Density Functional Theory Calculations,” *Phys. Chem. Chem. Phys.*, vol. 18, pp. 14509–14519, 2016.
- [4] L. Buannic, B. Orayech, J.-M. López Del Amo, J. Carrasco, N. A. Katcho, F. Aguesse, W. Manalastas, W. Zhang, J. Kilner, and A. Llordés, “Dual Substitution Strategy to Enhance  $\text{Li}^+$  Ionic Conductivity in  $\text{Li}_7\text{La}_3\text{Zr}_2\text{O}_{12}$  Solid Electrolyte,” *Chem. Mater.*, vol. 29, no. 4, pp. 1769–1778, 2017.
- [5] S. Plimpton, “Fast Parallel Algorithms for Short-Range Molecular Dynamics,” *J. Comput. Phys.*, vol. 117, no. 1, pp. 1 – 19, 1995.

- [6] A. Pedone, G. Malavasi, M. C. Menziani, A. N. Cormack, and U. Segre, “A New Self-Consistent Empirical Interatomic Potential Model for Oxides, Silicates, and Silica-Based Glasses,” *J. Phys. Chem. B*, vol. 110, no. 24, pp. 11780–11795, 2006.
- [7] D. Rettenwander, G. Redhammer, F. Preishuber Pflugl, L. Cheng, L. Mirara, R. Wagner, A. Welzl, E. Suard, M. M. Doeff, M. Wilkening, J. Fleig, and G. Amthauer, “Structural and Electrochemical Consequences of Al and Ga Cosubstitution in  $\text{Li}_7\text{La}_3\text{Zr}_2\text{O}_{12}$  Solid Electrolytes,” *Chem. Mater.*, vol. 28, no. 7, pp. 2384–2392, 2016.